

Short communication

An investigation of polypyrrole–LiV₃O₈ composite cathode materials for lithium-ion batteries

C.Q. Feng^{a,c}, S.Y. Chew^{a,b}, Z.P. Guo^{a,b,*}, J.Z. Wang^{a,b}, H.K. Liu^{a,b}

^a Institute for Superconducting and Electronic Materials, University of Wollongong, NSW 2522, Australia

^b ARC Centre of Excellence for Electromaterials Science, University of Wollongong, NSW 2522, Australia

^c Faculty of Chemistry and Material Sciences, Hubei University, 430062 Wuhan, China

Available online 30 June 2007

Abstract

A novel lithium trivanadate/polypyrrole (LiV₃O₈–PPy) composite, suitable for lithium-ion battery cathodes, was synthesized by dispersing LiV₃O₈ and PPy powders in ethanol followed by heating. The polypyrrole acts as a conducting matrix, a binder and an active material, as well as a volume change buffer agent, which holds the LiV₃O₈ particles in place during the charge/discharge cycles. The new material was characterized by scanning electron microscopy. It was found that polypyrrole particles were uniformly distributed among the LiV₃O₈ powders, which could significantly enhance the electrical conductivity and stability of the composite electrode. The composite containing 20 wt% PPy exhibits a good reversibility, higher coulombic efficiency and better cycle life than the bare LiV₃O₈ electrode.

© 2007 Published by Elsevier B.V.

Keywords: LiV₃O₈; Polypyrrole; Lithium-ion battery; Cyclability

1. Introduction

Layered trivanadate, LiV₃O₈, as a species of the lithiated vanadate family, has been widely studied as a cathode material for lithium-ion batteries due to its attractive characteristics, such as high specific energy, good rate capacity and long cycle life [1–4]. It is well known that the preparation method for LiV₃O₈ strongly influences its electrochemical properties, such as discharge capacity, rate capacity and cycle performances. Traditional synthesis of LiV₃O₈ is carried out by reacting Li₂CO₃ and V₂O₅ at 680 °C for 10 h [5,6]. This method usually produces sintered LiV₃O₈ with the low capacity of 180 mAh g^{−1} in the range of 1.8–4.0 V. To improve the electrochemical performance of LiV₃O₈, a great deal of research has been focused on the preparation method, for example, Xu et al. [7] synthesized LiV₃O₈ nanorods with an initial discharge capacity of 302 mAh g^{−1} by using a hydrothermal reaction method; West et al. [8] obtained a finely dispersed form of LiV₃O₈ through dehydration of aqueous lithium vanadate gel and the synthesized LiV₃O₈ showed a high capacity and good reversibil-

ity. More recently, Yang et al. [9] developed an economical microwave route for the synthesis of electrochemically active LiV₃O₈ materials and also investigated the influence of irradiation power, reaction time and temperature on the electrochemical performance of the LiV₃O₈. In our previous study [10], it was found that the LiV₃O₈ material synthesized through a rheological phase reaction, using citric acid as the complexing agent, delivered a discharge capacity of 256 mAh g^{−1} with very good reversibility. However, since electrical conductivity and viscosity of the as-prepared LiV₃O₈ powders are very low, the cathode materials must be well combined with a conductive agent and binding materials when preparing an electrode. Normally, carbon black is used as the electrical conductor in electrodes, while PVDF or PTFE is used as the binder. The total amount of carbon black and binder must be more than 15% of the total weight of electrode materials to maintain the good conductivity and mechanical stability of the cathodes. In order to reduce the inert weight of carbon black and binder, the use of electronically conducting polymers which have both binding and conducting functions, such as polypyrrole (PPy), has been proposed. The electronically conducting polymer, PPy, was also found to be electrochemically active for lithium-ion insertion and extraction in the voltage range of 2.0–4.5 V versus Li/Li⁺ and had a theoretical capacity of 72 mAh g^{−1} [11]. Therefore, polypyrrole additives can be used as conductive agents and as binders, as

* Corresponding author at: Institute for Superconducting and Electronic Materials, University of Wollongong, NSW 2522, Australia. Tel.: +61 2 4221 5727; fax: +61 2 4221 5731.

E-mail address: zguo@uow.edu.au (Z.P. Guo).

well as active materials in the cathode of lithium-ion batteries. A series of electrode material-conducting polymer composites have been investigated, such as MnO_2/PPy , $\text{LiMn}_2\text{O}_4/\text{PPy}$, $\text{V}_2\text{O}_5/\text{PPy}$, $\text{V}_2\text{O}_5/\text{polyaniline}$, Si-PPy , etc. [12–16] however, using polypyrrole powder as an additive for a LiV_3O_8 cathode has not been explored.

In this work, we attempted to incorporate polypyrrole into LiV_3O_8 and to prepare a novel organic–inorganic composite, $\text{LiV}_3\text{O}_8\text{-PPy}$, with the aim of improving the electrochemical performance of LiV_3O_8 cathode. The electrochemical properties of $\text{LiV}_3\text{O}_8\text{-PPy}$ as a cathode material were systematically investigated.

2. Experimental

2.1. Materials preparation

Lithium trivanadate, LiV_3O_8 , was prepared by a rheological phase reaction. The starting materials were analytically pure LiOH , V_2O_5 and citric acid. LiOH , V_2O_5 and citric acid were mechanically mixed in a molar ratio of 1:1.5:4.8 in an agate mortar. After the mixture was ground homogeneously, an appropriate amount of water was added to the resultant powder to obtain a rheological state mixture. The mixture was then heated at 90°C for 12 h. After that, the precursor was sintered at 480°C for 12 h to form the expected product. The conductive polypyrrole was prepared via oxidative chemical polymerization. The liquid pyrrole monomer, sodium *p*-toluenesulfonate was dispersed in deionised water. The solution was then magnetically stirred at 5°C for 6 h to complete the polymerization reaction.

The composite powder of $\text{LiV}_3\text{O}_8\text{-PPy}$ was prepared as follows: the as-prepared polypyrrole powder was first dispersed in ethanol in an ultrasonic bath for 30 min, then as-prepared LiV_3O_8 powder was added in. After an additional 2 h holding period in the ultrasonic bath, the composite powder was dried at 40°C and then heated at 110°C for 4 h.

2.2. Characterization of samples

The micromorphology of LiV_3O_8 and $\text{LiV}_3\text{O}_8\text{-PPy}$ composites was observed using a JEOL JSM 6460A scanning electron microscope (SEM). Electrochemical measurements of the $\text{LiV}_3\text{O}_8\text{-PPy}$ and bare LiV_3O_8 were accomplished by assembling CR2032 coin cells. The cathodes were prepared by mixing 85 wt% active materials ($\text{LiV}_3\text{O}_8\text{-PPy}$ or bare LiV_3O_8) with 10 wt% carbon black and 5 wt% PVDF (polyvinylidene fluoride) solution. The active materials and carbon black powders were first added to a solution of PVDF in *N*-methyl-2-pyrrolidinone (NMP) to make a slurry with appropriate viscosity. The slurry was then spread on aluminum foil to make the electrode. After the electrode was dried at 100°C for 2 h in vacuum, it was compressed at a rate of about 150 kg cm^{-2} . Coin cells were assembled in an argon filled glove box, where the counter electrode was Li metal and the electrolyte was 1 M LiPF_6 dissolved in a 50/50 vol% mixture of ethylene carbonate (EC) and dimethyl carbonate (DMC). These cells were cycled between 1.5 and 3.85 V at a constant current density of 40 mA g^{-1} at

room temperature to measure the electrochemical response. Ac impedance measurements were carried out utilizing a CHI 660B electrochemical workstation. Electrochemical impedance measurements were carried out in the open circuit voltage state by applying an ac voltage of 5 mV over the frequency range from 1 mHz to 100 kHz.

3. Results and discussion

SEM analysis was conducted on the $\text{LiV}_3\text{O}_8\text{-PPy}$ composite containing 80 wt% LiV_3O_8 to analyse the microstructure. Fig. 1 compares the microstructures of LiV_3O_8 and $\text{LiV}_3\text{O}_8\text{-PPy}$ powders. It can be seen that the morphology of the LiV_3O_8 powders (Fig. 1(a)) comprises needle-like or flake-like structures which have very sharp edges. In the case of $\text{LiV}_3\text{O}_8\text{-PPy}$ composites (Fig. 1(b)), most of the PPy particles with particle sizes around $1\ \mu\text{m}$ are agglomerates, which are distributed among the LiV_3O_8 powders. Fig. 1(c) is a low magnification view of $\text{LiV}_3\text{O}_8\text{-PPy}$ composites, where it can be seen that porous PPy powders are well dispersed in the LiV_3O_8 powders. EDX mapping of the different elements was conducted to analyse the distribution of the species within the particles (Fig. 2). The bright spots correspond to the presence of each element. Based on the EDX elemental maps, V, O and N in the sample are homogeneously distributed in the composite, indicating uniform distribution of LiV_3O_8 and PPy.

Fig. 3 shows the specific discharge capacity of the electrodes prepared with $\text{LiV}_3\text{O}_8\text{-PPy}$ composite and bare LiV_3O_8 upon cycling. Capacity fading was observed after several charge/discharge cycles in all cases, but the decay of the discharge capacity for $\text{LiV}_3\text{O}_8\text{-PPy}$ composite electrodes with 15% or 20% PPy was far slower compared to the bare LiV_3O_8 cathode. In particular, the $\text{LiV}_3\text{O}_8\text{-20\%PPy}$ electrode shows stable cyclability with only 0.4% capacity loss/cycle. The reversible capacity of $\text{LiV}_3\text{O}_8\text{-PPy}$ electrode is also higher than that of the bare LiV_3O_8 electrode with $\text{LiV}_3\text{O}_8\text{-20\%PPy}$ electrode showing an initial capacity of 292 mAh g^{-1} .

To explore the reasons for capacity fading and directly analyse any changes in the microstructure or morphology of the particles during cycling, the electrodes fabricated from the bare LiV_3O_8 and $\text{LiV}_3\text{O}_8\text{-PPy}$ composites containing 20% PPy were observed after cycling with SEM. Fig. 4(a) is a SEM image showing the surface of the LiV_3O_8 electrode after 30 cycles, where big cracks can be clearly observed on the surface of the electrode. However, for the $\text{LiV}_3\text{O}_8\text{-PPy}$ composite electrode (Fig. 4(b)), the cracks are not so obvious and the integrity of electrode is retained, suggesting good structural stability of the composite electrode. This excellent stability of the electrode may be attributed to the existence of well-dispersed PPy particles within the LiV_3O_8 powders. The LiV_3O_8 volume change during charging/discharging could be buffered by the presence of PPy. In addition, PPy could work as an efficient host matrix to prevent cracking and pulverization of the LiV_3O_8 electrode. At the same time, PPy can also act as a conductive binder, increasing the contact between particles. To verify this concept, ac impedance measurements were conducted. The Nyquist plots obtained for $\text{LiV}_3\text{O}_8\text{-PPy}$ composite electrode compared with LiV_3O_8 elec-

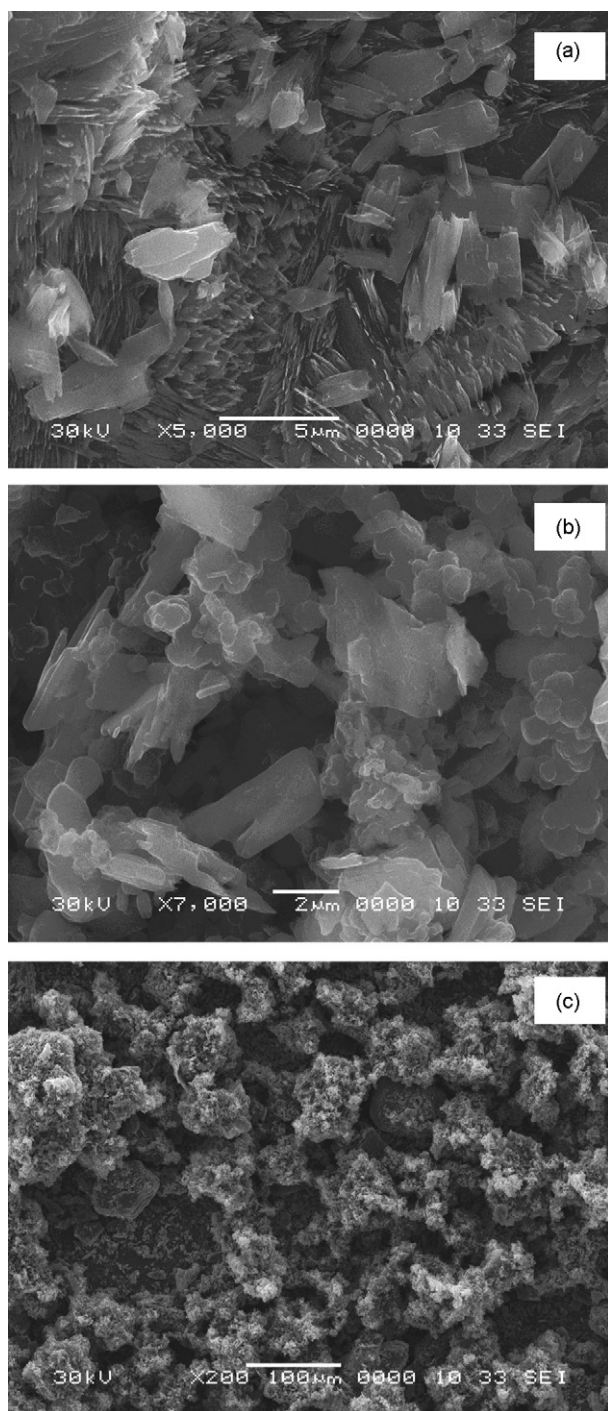


Fig. 1. SEM images of (a) LiV_3O_8 powder; (b) LiV_3O_8 -PPy at higher magnification; (c) LiV_3O_8 -PPy at lower magnification.

trode in the OCV state are shown in Fig. 5. The thickness of the electrodes was controlled at $50\ \mu\text{m}$ and the coated area of the electrodes at $1\ \text{cm}^2$. Just one semicircle was observed for both samples. In the low frequency region a straight line was obtained which represents the combination of diffusion and capacitance behavior in the solid electrode. The diameter of the semicircle for LiV_3O_8 -PPy composite electrode ($130\ \Omega$) is much smaller compared with that of bare LiV_3O_8 electrode ($400\ \Omega$). It has been reported that such a semicircle might contain a contribution

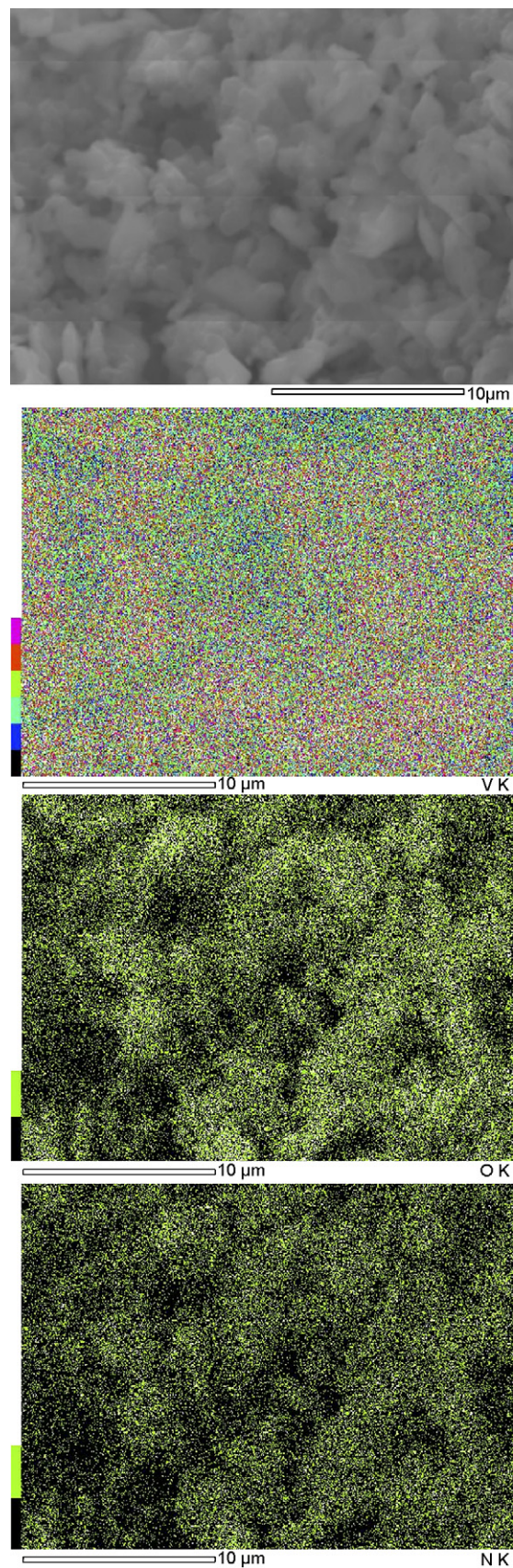


Fig. 2. SEM and chemical map of V, O and N for the LiV_3O_8 -PPy composite powder.

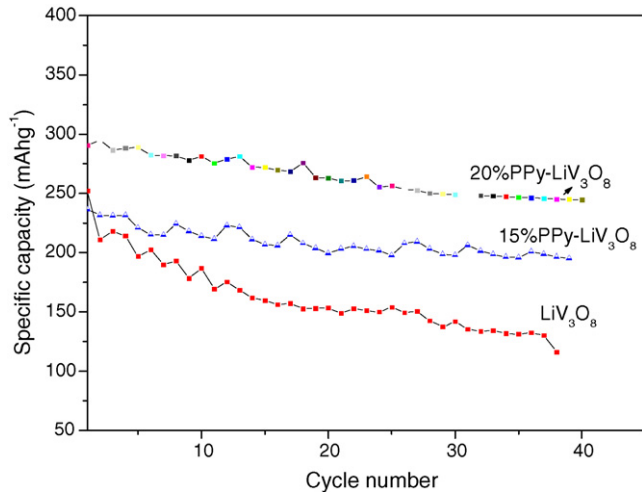


Fig. 3. Capacity as a function of cycle number for the bare LiV₃O₈ electrode and LiV₃O₈-PPy composite electrode.

due to the compaction of particles in the cathode, i.e. the inter-particle contacts such as LiV₃O₈-PPy-carbon or carbon-carbon contacts. Therefore, the reduction in the diameter of the semi-circle in LiV₃O₈-PPy composite electrodes probably can be ascribed to a decrease in the inter-particle contact resistance.

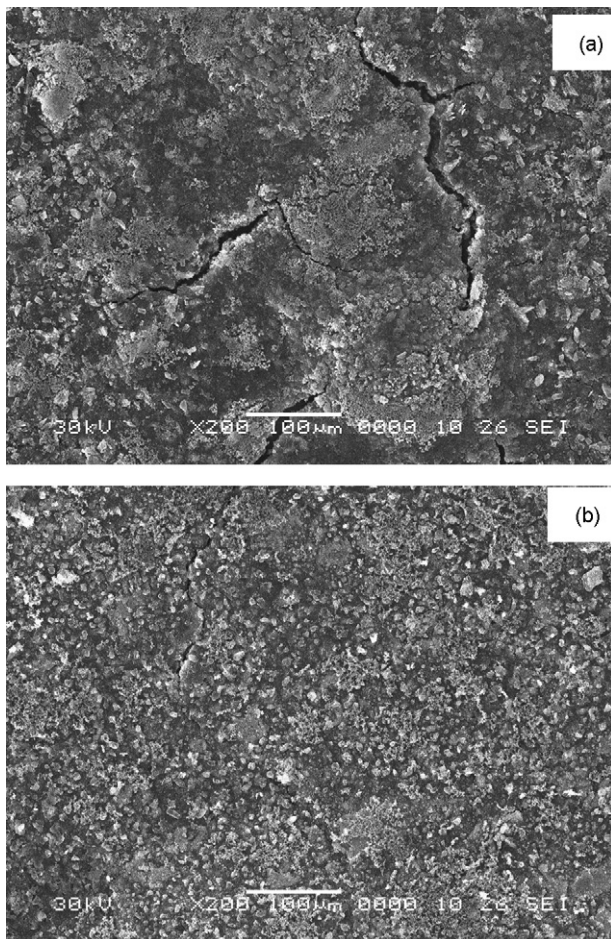


Fig. 4. SEM images of the electrode after 30 cycles: (a) the bare LiV₃O₈ electrode and (b) LiV₃O₈-PPy composite electrode.

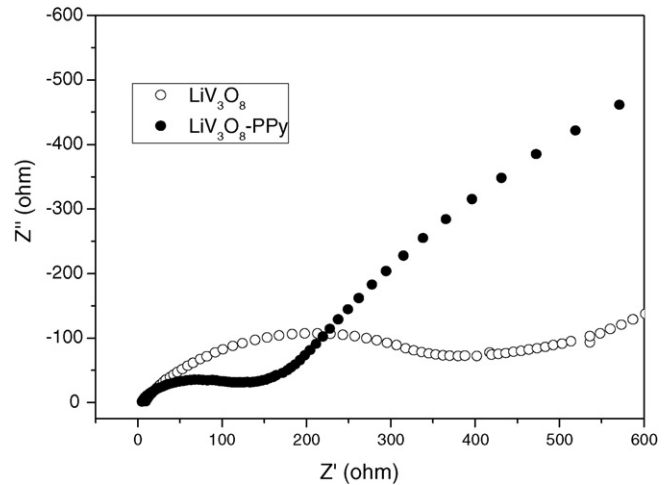


Fig. 5. Impedance plots for the cathodes of LiV₃O₈ and LiV₃O₈-PPy composite.

Thus, it can be speculated that the polypyrrole works well as both a conducting agent and a binder.

Fig. 6 compares the charge/discharge curves of the 2nd, the 5th and the 10th cycles for the composite and pure LiV₃O₈ electrodes. There are several plateaus in the voltage profiles for the

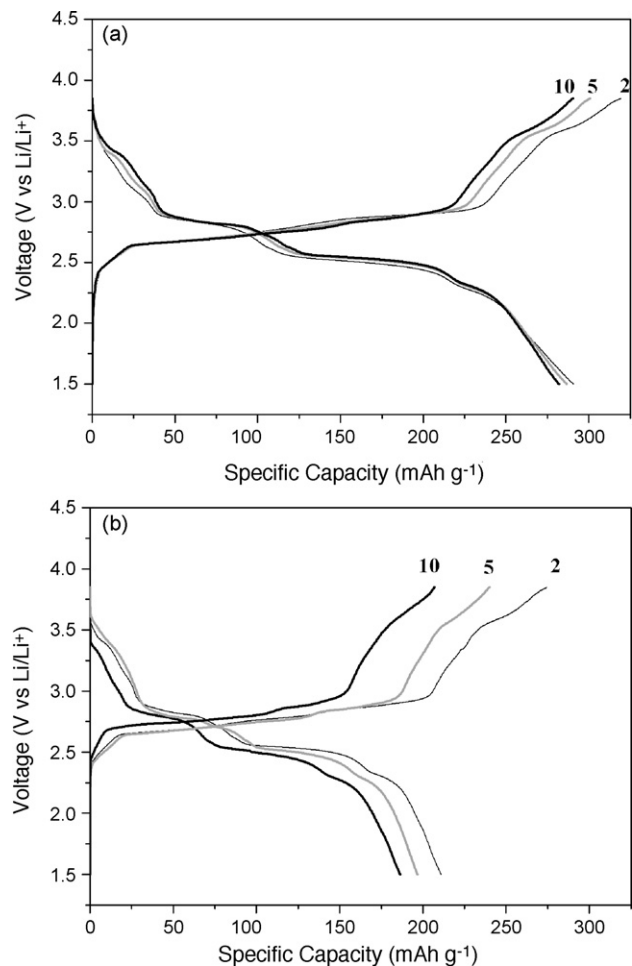


Fig. 6. The 2nd, 5th and 10th charging/discharging curves of (a) the LiV₃O₈-PPy composite electrode and (b) the bare LiV₃O₈ electrode.

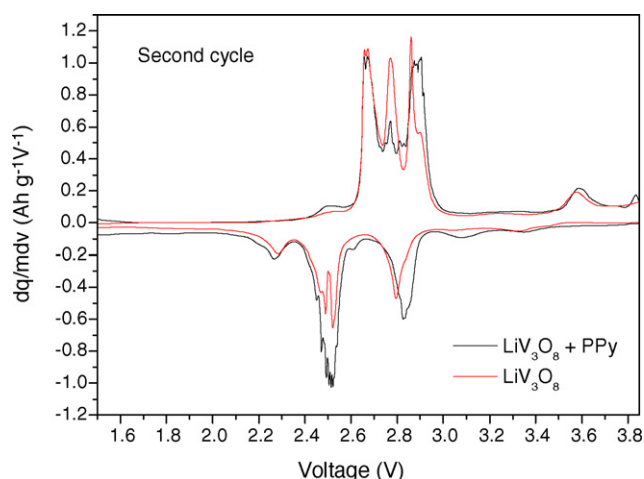


Fig. 7. Differential capacity vs. voltage plots for the bare LiV_3O_8 electrode and LiV_3O_8 -PPy composite electrode.

lithium intercalation and deintercalation of LiV_3O_8 -PPy electrodes (Fig. 6(a)), which is quite similar to that of the LiV_3O_8 electrodes (Fig. 6(b)). The “differential capacity (dq mdV^{-1})” plots calculated from the voltage variation are also shown in Fig. 7, as these curves emphasize the details of the voltage curves.

Generally, there are five pairs of peaks in the differential capacity plots, which correspond to the plateaus in the charge/discharge curves. The sharp peaks indicate that the lithium insertion/deintercalation proceeds through a few multiphase regions until the limit for reversible lithium uptake is reached. The intensity of the cathodic peak of the LiV_3O_8 -PPy electrode is much higher than that for the bare LiV_3O_8 electrode, indicating the higher discharge capacity of LiV_3O_8 -PPy electrode. It is also found that the coulombic efficiency for LiV_3O_8 -PPy composite electrode is higher when compared to the bare LiV_3O_8 cathode. It is well known that polypyrrole serves the dual-purpose of a binder and a conducting additive when used with cathode powders such as MnO_2 , LiMn_2O_4 and V_2O_5 [12–15]. In our studies, the roles of PPy in the cathodes could be: (1) the polypyrrole in LiV_3O_8 -PPy composites is a conducting polymer, which could increase the conductivity of the samples; (2) PPy forms a matrix in which LiV_3O_8 particles are bound together, therefore, the particle-to-particle resistance will be decreased, thus reducing the irreversible reactions with the electrolyte; (3) PPy is an effective component that buffers the volume change of LiV_3O_8 during charge/discharge cycles; (4) PPy could also act as an efficient host matrix to prevent cracking and pulverization of the LiV_3O_8 electrode due to

phase transitions, thus improving the cyclability of the LiV_3O_8 electrode.

4. Conclusions

A novel composite of LiV_3O_8 powder coated with conducting polypyrrole can be prepared by a simple dispersion method. The cathode materials had higher capacities and substantially improved cyclability compared to bare LiV_3O_8 cathodes. The vast network of the PPy matrix is a suitable environment to increase the electrical conductivity and prevent cracking and pulverization of the LiV_3O_8 electrode. The composite showed good electrochemical properties in rechargeable lithium cells.

Acknowledgments

The authors would like to thank Dr. K. Konstantinov for his help in the SEM measurements. Financial support from the Australian Research Council is gratefully acknowledged.

References

- [1] L.A. de Picciotto, K.T. Adendorff, D.C. Liles, M.M. Thackeray, *Solid State Ionics* 62 (1993) 297.
- [2] M. Manev, A. Momchilov, A. Nassalevska, G. Pistoia, M. Pasquali, *J. Power Sources* 54 (1995) 501.
- [3] G. Pistoia, M. Panero, M. Tocci, R.V. Moshtev, V. Manev, *Solid State Ionics* 13 (1984) 311.
- [4] M. Pasquali, G. Pistoia, V. Manev, R.V. Moshtev, *J. Electrochem. Soc.* 133 (1986) 2454.
- [5] G. Pistoia, S. Panero, M. Tocci, R. Moshtev, V. Manev, *J. Solid State Ionics* 13 (1984) 12.
- [6] G. Pistoia, M. Pasquali, M. Tocci, V. Manev, R. Moshtev, *J. Power Sources* 15 (1985) 13.
- [7] H.Y. Xu, H. Wang, Z.Q. Song, Y.W. Wang, H. Yan, M. Yoshimura, *Electrochim. Acta* 49 (2004) 349.
- [8] K. West, B.Z. Christiansen, S. Skaarup, Y. Saidi, J. Barker, I.I. Olsen, R. Pynenburg, R. Koksang, *J. Electrochem. Soc.* 143 (1996) 820.
- [9] G. Yang, G. Wang, W. Hou, *J. Phys. Chem. B* 109 (2005) 11186.
- [10] C.Q. Feng, L.F. Huang, Z.P. Guo, J.Z. Wang, H.K. Liu, *J. Power Sources*, in press.
- [11] T. Osaka, T. Momma, K. Nishimura, S. Kakuda, T. Ishii, *J. Electrochem. Soc.* 141 (1994) 1994.
- [12] S. Kuwabata, A. Kisimoto, T. Tanaka, H. Yoneyama, *J. Electrochem. Soc.* 141 (1994) 10.
- [13] M. Nishizawa, K. Mukai, S. Kuwabata, C.R. Martin, H. Yoneyama, *J. Electrochem. Soc.* 144 (1997) 1923.
- [14] S. Kuwabata, T. Idzu, C.R. Martin, H. Yoneyama, *J. Electrochem. Soc.* 145 (1998) 2707.
- [15] F. Huguénin, E.M. Girotto, R.M. Torresi, D.A. Buttry, *J. Electroanal. Chem.* 536 (2002) 37.
- [16] Z.P. Guo, J.Z. Wang, H.K. Liu, S.X. Dou, *J. Power Sources* 146 (2005) 448.